PHYSICAL REVIEW B **86**, 241201(R) (2012)

Effects of confinement and environment on the electronic structure and exciton binding energy of MoS_2 from first principles

Hannu-Pekka Komsa[1] and Arkady V. Krasheninnikov[1,2]

[1]*Department of Physics, University of Helsinki, P.O. Box 43, 00014 Helsinki, Finland*

[2]*Department of Applied Physics, Aalto University, P.O. Box 1100, 00076 Aalto, Finland*

(Received 10 August 2012; revised manuscript received 2 October 2012; published 7 December 2012)

Using GW first-principles calculations for few-layer and bulk MoS_2, we study the effects of quantum confinement on the electronic structure of this layered material. By solving the Bethe-Salpeter equation, we also evaluate the exciton energy in these systems. Our results are in excellent agreement with the available experimental data. Exciton binding energy is found to dramatically increase from 0.1 eV in the bulk to 1.1 eV in the monolayer. The fundamental band gap increases as well, so that the optical transition energies remain nearly constant. We also demonstrate that environments with different dielectric constants have a profound effect on the electronic structure of the monolayer. Our results can be used for engineering the electronic properties of MoS_2 and other transition-metal dichalcogenides and may explain the experimentally observed variations in the mobility of monolayer MoS_2.

DOI: 10.1103/PhysRevB.86.241201 PACS number(s): 71.35.Cc, 71.20.Ps, 73.22.−f

I. INTRODUCTION

Similar to graphite and hexagonal boron nitride (h-BN), layered transition-metal dichalcogenides (TMDs) are van der Waals bonded materials which can also exist as monolayers. The prototypical TMD, molybdenum disulfide (MoS_2), is a semiconductor with good electronic[1,2] and mechanical characteristics,[3,4] which can be used as a dry lubricant[5,6] and in the industrial hydrodesulfurization process.[7] Recently, two-dimensional sheets of MoS_2 have received a considerable amount of attention owing to the advances in the monolayer production by either exfoliation from the bulk system[2,8–10] or direct growth methods.[11–13] Nanostructured MoS_2 systems have shown good potentials in nanoelectronic,[2,14] flexible electronic,[3,15] and photonic[10,16–18] applications.

For these applications, detailed knowledge of the electronic structure is of critical importance. The band structure of bulk MoS_2 is fairly well known, as are the fundamental band gap E_g ($E_g = I - A$, where I and A are the ionization potential and the electron affinity, respectively), optical transitions, and exciton properties.[19–22] Recent experimental studies of monolayer and few-layer MoS_2 have demonstrated a transition from indirect gap to direct gap at the monolayer limit and the evolution of the optical transitions.[16,23,24] The fundamental band gap of few-layer MoS_2 cannot directly be obtained from optical experiments. Several GW calculations have reported a monolayer gap clearly higher than for the bulk system, although the calculated results vary widely between 2.0 and 3.0 eV.[25–30] At the same time, the effects of quantum confinement on the electronic structure of MoS_2 are not fully understood. The dimensionality of the system may strongly modify the exciton properties.[31] The exciton binding energy connects the optical transitions to fundamental band gaps, but with the information on the gap value missing, the binding energies for monolayer and few-layer cases cannot be deduced either. Finally, if the dimensionality indeed plays a major role in defining the fundamental band gap and exciton binding energy, it is of interest to examine how different environments could alter these properties. This issue has not previously been explored in the context of two-dimensional materials, although it has been seen to affect the conductivity of the system.[2,16,32]

In this Rapid Communication, by using advanced first-principles calculations, we provide a consistent picture of the effects of confinement on the electronic structure from bulk to few-layer MoS_2 and address the above-mentioned issues. In particular, (i) we provide an explanation for the contradicting results of previous calculations and obtain accurate data for the fundamental gap in few-layer MoS_2, (ii) we calculate optical transition energies, which are nearly constant for the structures, in agreement with the experiments, and demonstrate that while the exciton binding energy is only about 0.1 eV for bulk MoS_2, it increases to 1.1 eV in the monolayer limit, and (iii) we show that the environment with a high dielectric constant in monolayer MoS_2 decreases the fundamental band gap and also reduces exciton binding energy.

II. METHODS

In all our calculations, we used the density functional theory in the framework of plane-wave projector-augmented wave (PAW) formalism as implemented in the VASP package.[34,35] All calculations were carried out with a primitive cell, as illustrated in Fig. 1(a). The **k**-point mesh in the lateral directions was always 12×12, whereas for the perpendicular direction three **k** points were used for bulk and the number was reduced to one closer to the monolayer limit. The plane-wave cutoff is 500 eV. Test calculations with larger number of **k** points and higher cutoff energies gave essentially the same results. At the semilocal level, we used the Perdew-Burke-Ernzerhof (PBE) exchange-correlation functional,[36] which yields the in-plane lattice constant $a = 3.18$ Å, which is in good agreement with the experimental value $a = 3.16$ Å.[37] The van der Waals interactions were accounted for through dispersion correction on top of PBE (PBE-D)[38] which brings the calculated perpendicular lattice constant ($c/a = 3.91$) very close to the experimental value ($c/a = 3.89$).

The G_0W_0 calculations were performed on top of the PBE wave functions at the PBE-optimized geometry. The

 ©2012 American Physical Society

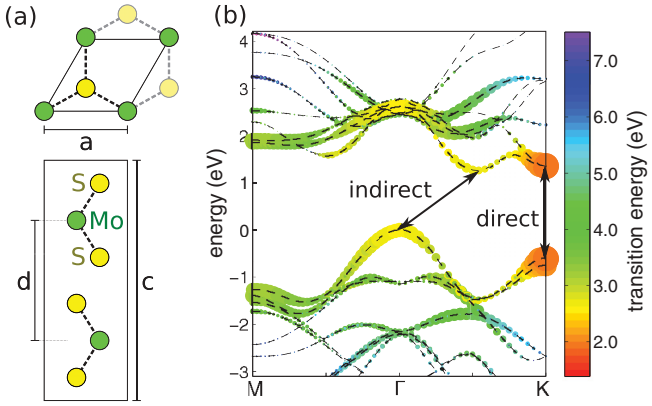

FIG. 1. (Color online) (a) Schematic representation of the geometry of bulk MoS_2 with top and side views. (b) Band structure of bulk MoS_2 and the dominant transition matrix elements for direct transitions. Each transition corresponds to a pair of valence and conduction band states, which are then denoted according to the energy and strength of the transition. The radius of the circle (or width of the line) represents the magnitude of the matrix element,[33] and the color represents the respective transition energy.

plane-wave cutoff was 400 eV for wave functions and 200 eV for the response function. Full frequency-space integration was used for the latter. Including empty bands about 80 eV above Fermi level was found to be sufficient to yield converged quasiparticle energy differences.[39] A consistent description of the unoccupied state manifold in supercells of different sizes was guaranteed by increasing the number of unoccupied states in the calculation linearly with the supercell size c. Consequently, the highest unoccupied state is always at roughly the same energy with respect to the Fermi level of the system. The Bethe-Salpeter equation (BSE) was solved on top of the G_0W_0 quasiparticle spectrum. We also accounted for spin-orbit coupling. The eigenvalue shifts due to spin-orbit interaction were calculated at the PBE level and added *a posteriori* to the GW quasiparticle energies. Full inclusion of spin-orbit effects at the GW level is expected to be within a few tens of meVs, as indicated by selected test calculations.

III. RESULTS

The band structure for bulk MoS_2 is given in Fig. 1(b). The experimental gap is indirect (1.29 eV), with the valence-band maximum (VBM) being located at the Γ point and the conduction-band minimum (CBM) at the valley located about halfway between the Γ and K points.[40] The position of the VBM at the Γ point is sensitive to the interlayer interactions.[22,24,41,42] In the case of the monolayer, VBM at the Γ point moves below the K point, with a similar effect on the conduction band, and consequently, the gap becomes direct.[16] Experimentally, two strong excitonic transitions, called A and B, are observed at about 1.83–1.90 and 1.98–2.06 eV,[16,21,23] and they originate from transitions around the K point, as evident from the following observations: The A/B transition energies are fairly independent of the number of layers, in agreement with the behavior of the K point gap.[24] The calculated splitting of the VBM states at the K point due to spin-orbit coupling agrees with the separation between the A and B peaks.[30] Finally, from the magnitude of the optical matrix elements, as illustrated with circles of varying sizes in Fig. 1(b), the transitions at the K point dominate.

The calculated direct and indirect PBE gaps are shown in Fig. 2(a) as functions of the inverse interlayer distance $1/d$. The AB-stacked bulk MoS_2 structure [cf. Fig. 1(a)] corresponds to $1/d = 0.16$ Å^{-1}, whereas the $1/d \to 0$ limit corresponds to a monolayer. We also indicate the positions of the experimental gaps in bulk MoS_2, estimated by adding the exciton binding energy to the optical transition energy.[20,21] As the layer separation increases, the gaps quickly reach constant values as the interlayer overlap between electron clouds decreases. In the bulk limit, the PBE underestimates the band gaps by 0.4 eV, a common situation in the PBE calculations.

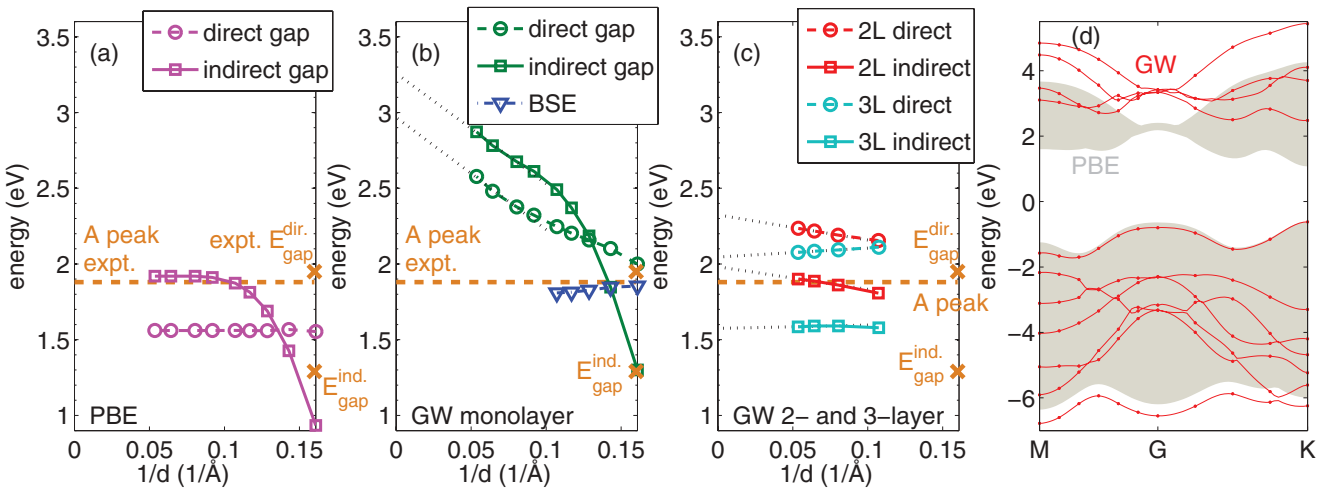

FIG. 2. (Color online) Band gaps and optical transition energies in bulk and few-layer MoS_2. Direct and indirect band gaps at (a) the PBE and (b) GW levels of theory. Exciton transition energies are also given in (b). (c) GW calculated gaps for bi- and trilayer cases. The dashed horizontal line corresponds to the experimental optical (A) transition,[21] and the crosses are for estimated bulk fundamental gaps.[20] (d) The extrapolated ($1/d \to 0$) GW band structure (red lines) overlayed on top of the PBE band structure (gray areas).

The GW approach is expected to yield more accurate gaps. Indeed, as shown in Fig. 2(b), in the bulk limit, the GW results are in excellent agreement with the experimental values. A curious behavior is seen with increasing interlayer distance, where the band gaps never reach a constant level. Instead, due to the nonlocal nature of the GW approximation, the gaps keep on increasing as $\sim 1/d$ (similar behavior has been observed for h-BN, Ref. 43), eventually leading to gaps much larger than in the case of PBE. In order to obtain the true monolayer band gaps, we extrapolate our results to the $1/d \rightarrow 0$ limit and obtain 3.0 eV. Without extrapolation, as evident from Fig. 2(b), a prohibitively large supercell in the perpendicular direction, or Coulomb cutoff techniques, would be needed for an accurate determination of the GW gaps of a monolayer. This also partly explains the variations in the GW results reported in the literature.[25–30] The large monolayer band gap is due to the interaction of an electron (or hole) with the induced surface (polarization) charge, which is repulsive in nature and thus leads to an increase in the gap value.[44] Such correlation effects are not accounted for at the PBE level of theory, consequently yielding a wrong band gap. Nevertheless, as shown in Fig. 2(d), the general features of the PBE band structure are still very similar to that obtained from the extrapolated GW results. For the monolayer, a constant shift of about 1.4 eV is required to align the PBE results to the GW ones, whereas it is only about 0.4 eV in the bulk case.

The fundamental band gap for monolayer MoS_2 calculated here is much larger than the measured energies for the A/B excitons. Naturally, fundamental band gaps obtained from the GW approach should not be compared with optical transition energies due to the missing electron-hole interaction (excitonic effects). For proper comparison with the experiments, we have calculated the optical transition energies through BSE. These results are also shown in Fig. 2(b). In contrast to the large variation in the K-point gaps, these transitions are nearly independent of the interlayer distance. Since exciton is a neutral entity (and the electron and hole are both localized in the Mo layer, as our analysis indicates), there is no significant surface charge or other long-range correlation effects. This is again in agreement with the experimental observation of A/B peaks occurring at close energies in monolayer, few-layer, and bulk samples.[16] Accounting for the spin-orbit interaction, the value of the B transition should be different from that of the A transition by splitting of the valence-band maximum at the K point. Our calculations at the PBE level of theory gave a VBM splitting of 0.15–0.20 eV (varying with the number of layers). This value is in a very good agreement with the experimental difference between A and B transition energies (0.15–0.18 eV).[16,21] The BSE approach was found to modify these shifts by less than 20 meV.[30] We note that an accurate band structure is a prerequisite for obtaining reliable BSE results. Thus, good agreement with experiment for the excitons also gives credence for the quality of our calculated fundamental G_0W_0 gaps. The calculated exciton binding energy in the bulk is 0.13 eV, in good agreement with the experimental value of 0.08 eV.[20] In contrast, for the monolayer MoS_2, we find a binding energy as high as 1.1 eV. The larger values of exciton binding energies in monolayer MoS_2 with respect to the bulk system are in line with the values reported for other low-dimensional systems:

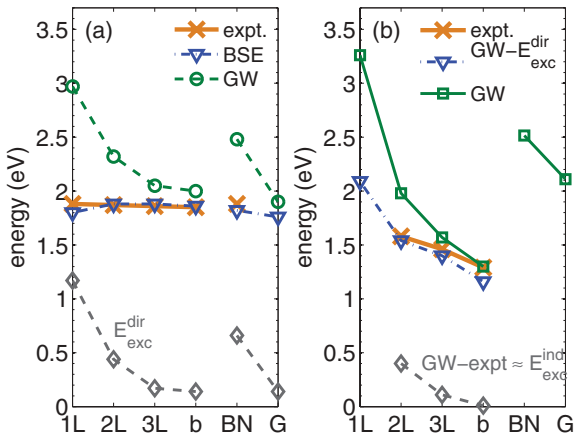

FIG. 3. (Color online) Comparison of calculated and experimental[16,50] (a) direct and (b) indirect gaps. The calculated gaps are obtained through extrapolation of the results shown in Figs. 2(b) and 2(c). The labels 1L, 2L, and b stand for monolayer, bilayer, and bulk MoS_2, while BN and G correspond to a monolayer MoS_2 deposited on BN and a graphene sheet. E_{exc} stands for exciton binding energy.

graphane,[45] BN,[46] graphene,[47] and carbon nanotubes.[48,49] An increase in binding energy for monolayer was also predicted in previous calculations.[29,30]

Having obtained results for the bulk and the monolayer limits, we further study how the dimensionality affects the results. It is of interest to consider systems of few-layer MoS_2, for which the experimental results are also available.[16] The band gaps, as shown in Fig. 2(c), still scale as $1/d$, although with a smaller prefactor. It is evident that with increasing number of layers, both the direct and indirect extrapolated band gaps approach the bulk values, as expected. For the bilayer, the band gaps are still clearly higher than the respective bulk gaps, but for the trilayer the difference is already minor.

In order to better visualize the trends when the number of layers changes, we plot in Fig. 3(a) the experimental and calculated optical transition energies together with the extrapolated fundamental G_0W_0 band gaps at the K point. The optical transitions are again found at nearly constant energies, in good agreement with the experimental results.[16] On the other hand, the fundamental gaps with increasing number of layers vary strongly. Both the gaps and the exciton binding energies are seen to quickly approach the bulk values. The electron/hole interaction with the surface charge decreases with increasing thickness of the material.[44]

Another way to decrease the interaction with the surface charge is to alter the dielectric environment of the MoS_2 sample. We examine these effects by introducing a monolayer of graphene or BN next to a monolayer of MoS_2. We are only interested in finding model systems with different dielectric environments and do not try to mimic real G/MoS_2 or BN/MoS_2 systems. Therefore, to speed up the calculations, we employ primitive cells where the graphene or BN monolayer is stretched to obtain lattice matching with MoS2, yet the characteristic metallic and insulating behaviors of graphene and BN are still retained. The results of these calculations are also given in Fig. 3. Already with BN, there is a clear decrease of the MoS_2 gap, but due to the low dielectric

TABLE I. The calculated and the available experimental optical gaps, fundamental gaps, and exciton binding energies for bulk and monolayer (ML) MoS_2, $MoSe_2$, and $MoTe_2$. The experimental data are collected from Refs. 20,21,54, and 55 for MoS_2, Refs. 21,55, and 56 for $MoSe_2$, and Refs. 21,55, and 57 for $MoTe_2$. Indirect gaps are from Ref. 37. The experimental fundamental gap is obtained by adding the exciton binding energy to the optical transition ($A + E_{exc}$).

	MoS_2		$MoSe_2$		$MoTe_2$	
	Bulk	ML	Bulk	ML	Bulk	ML
			Optical transition A			
BSE	1.86	1.80	1.55	1.64	1.08	1.17
Experimental	1.88	1.88	1.57		1.10	
			Fundamental gap			
GW direct	2.00	2.97	1.66	2.41	1.15	1.79
Experimental ($A + E_{exc}$)	1.96		1.64		1.24	
GW indirect	1.30	3.26	1.11	2.97	0.88	2.49
Experimental indirect gap	1.29		1.10		1.00	
			Exciton binding energy			
Calculated	0.13	1.1	0.11	0.78	0.07	0.62
Experimental	0.08		0.07		0.14	

constant of BN, the gap is still far from the bulk value. The large dielectric constant of graphene, on the other hand, leads to fundamental band gaps similar to bulk MoS_2. Different dielectric environments can thus be used to engineer the fundamental band gap in MoS_2 and likely in other TMDs.

The experimental indirect band gaps for MoS_2 as a function of the number of layers were also reported in Ref. 16. These are presented in Fig. 3(b) together with the calculated results. The GW fundamental gaps are again clearly higher than the measured optical gaps. In fact, the exciton binding energies, when evaluated from the difference between calculated fundamental gaps and experimental optical transitions, appear to be very similar to the case of a direct exciton. Furthermore, in Ref. 29, indirect exciton binding energy of a bilayer was estimated to be only 0.1 eV higher than for the corresponding direct exciton, which is due to different effective masses. The difference is likely to be somewhat larger for a monolayer case but even smaller for few-layer cases. Thus, we also show in Fig. 3(b) the results for indirect optical transition energies obtained by taking the indirect GW band gap and subtracting from it the *direct* exciton binding energy. The results agree well with the experimental data.[16,51] The indirect fundamental gap and exciton binding energy are similarly affected by the dielectric environment.

As mentioned above, although the optical gap is well known experimentally, it is difficult to directly probe the fundamental band gap. The large monolayer exciton binding energy leads to a short exciton decay time ($\tau \sim 1/E_{exc}$)[52] and can thus explain the observation of the much improved photoluminescence yield in the free-standing regions vs on-substrate regions.[16] On the other hand, the changes in the fundamental gaps induced by quantum confinement and dielectric environment in few-layer MoS_2 should be observable in the conductivity of these systems. In reality, it may be difficult to isolate these effects from those due to the quality of the contacts, charged defects in the substrate, or screening of defects in the monolayer by the environment.[53] Then again, deposition of a high dielectric constant layer on top of a MoS_2 monolayer has yielded a significant increase in the mobility[2,18] when compared to results obtained for a monolayer surrounded by vacuum or silica.[8,32] On the basis of our calculated results, one possible explanation could be the smaller fundamental gap caused by the high dielectric constant environment.

In order to understand if the trends observed for MoS_2 are general for semiconductor TMD materials, we also calculated the fundamental gaps and exciton binding energies in $MoSe_2$ and $MoTe_2$ monolayers and bulk systems. Exciton binding energies in monolayers proved to be in agreement with the results of previous calculations.[30] For bulk systems, the calculated (PBE-D) lattice constants (experimental ones follow in parentheses)[37] are $a = 3.32$ Å (3.30 Å) and $c/a = 3.92$ (3.92) for $MoSe_2$ and $a = 3.55$ Å (3.52 Å) and $c/a = 3.93$ (3.97) for $MoTe_2$. We stress that the electronic structure of bulk systems was found to be fairly sensitive to the lattice constants. In Table I, we present our simulation results for the bulk and monolayer for the molybdenum dichalcogenides and compare them to the experimental values. The agreement between the theoretical and experimental data is good, indicating that the trend is common, at least for molybdenum-family dichalcogenides, and likely for all layered transition metal dichalcogenides and their alloys.[59]

IV. CONCLUSIONS

In conclusion, using advanced first-principles methods, we calculated the quasiparticle band structure and the dominant optical transitions of few-layer and bulk MoS_2. Our results are in an excellent agreement with the available experimental data, thus justifying our computational approach. A dramatic increase in both the direct and indirect fundamental band gaps of the monolayer is found. The exciton binding energy is 0.1 eV for the bulk system and 1.1 eV for the monolayer. The band gap and exciton binding energy decrease with increasing number of layers in MoS_2 and other Mo-family dichalcogenides, as well as when a monolayer is surrounded by a high dielectric constant material. Different dielectric environments can thus be used to engineer the fundamental band gap in MoS_2 and other TMDs.

ACKNOWLEDGMENTS

We thank R. M. Nieminen and A. Gulans for fruitful discussions. We acknowledge financial support from the University of Helsinki Funds and the Academy of Finland through the COMP Centre of Excellence Grant and projects 218545 and 263416. We also thank CSC Finland for generous grants of computer time.

[1] R. Fivaz and E. Mooser, Phys. Rev. **163**, 743 (1967).
[2] B. Radisavljevic, A. Radenovic, J. Brivio, V. Giacometti, and A. Kis, Nat. Nanotechnol. **6**, 147 (2011).
[3] S. Bertolazzi, J. Brivio, and A. Kis, ACS Nano **5**, 9703 (2011).
[4] A. Castellanos-Gomez, M. Poot, G. A. Steele, H. S. J. van der Zant, N. Agrat, and G. Rubio-Bollinger, Adv. Mater. **24**, 772 (2012).
[5] J. M. Martin, C. Donnet, T. Le Mogne, and T. Epicier, Phys. Rev. B **48**, 10583 (1993).
[6] L. Cizaire, B. Vacher, T. L. Mogne, J. Martin, L. Rapoport, A. Margolin, and R. Tenne, Surf. Coat. Technol. **160**, 282 (2002).
[7] M. Daage and R. Chianelli, J. Catal. **149**, 414 (1994).
[8] K. S. Novoselov, D. Jiang, F. Schedin, T. J. Booth, V. V. Khotkevich, S. V. Morozov, and A. K. Geim, Proc. Nat. Acad. Sci. USA **102**, 10451 (2005).
[9] J. N. Coleman *et al.*, Science **331**, 568 (2011).
[10] G. Eda, H. Yamaguchi, D. Voiry, T. Fujita, M. Chen, and M. Chhowalla, Nano Lett. **11**, 5111 (2011).
[11] Y. Zhan, Z. Liu, S. Najmaei, P. M. Ajayan, and J. Lou, Small **8**, 966 (2012).
[12] K.-K. Liu, W. Zhang, Y.-H. Lee, Y.-C. Lin, M.-T. Chang, C.-Y. Su, C.-S. Chang, H. Li, Y. Shi, H. Zhang, C.-S. Lai, and L.-J. Li, Nano Lett. **12**, 1538 (2012).
[13] Y. Shi, W. Zhou, A.-Y. Lu, W. Fang, Y.-H. Lee, A. L. Hsu, S. M. Kim, K. K. Kim, H. Y. Yang, L.-J. Li, J.-C. Idrobo, and J. Kong, Nano Lett. **12**, 2784 (2012).
[14] H. Li, Z. Yin, Q. He, H. Li, X. Huang, G. Lu, D. W. H. Fam, A. I. Y. Tok, Q. Zhang, and H. Zhang, Small **8**, 63 (2012).
[15] J. Pu, Y. Yomogida, K.-K. Liu, L.-J. Li, Y. Iwasa, and T. Takenobu, Nano Lett. **12**, 4013 (2012).
[16] K. F. Mak, C. Lee, J. Hone, J. Shan, and T. F. Heinz, Phys. Rev. Lett. **105**, 136805 (2010).
[17] Z. Yin, H. Li, H. Li, L. Jiang, Y. Shi, Y. Sun, G. Lu, Q. Zhang, X. Chen, and H. Zhang, ACS Nano **6**, 74 (2012).
[18] H. S. Lee, S.-W. Min, Y.-G. Chang, M. K. Park, T. Nam, H. Kim, J. H. Kim, S. Ryu, and S. Im, Nano Lett. **12**, 3695 (2012).
[19] B. L. Evans and P. A. Young, Proc. Phys. Soc. **91**, 475 (1967).
[20] E. Fortin and F. Raga, Phys. Rev. B **11**, 905 (1975).
[21] A. R. Beal and H. P. Hughes, J. Phys. C **12**, 881 (1979).
[22] S. W. Han, G.-B. Cha, E. Frantzeskakis, I. Razado-Colambo, J. Avila, Y. S. Park, D. Kim, J. Hwang, J. S. Kang, S. Ryu, W. S. Yun, S. C. Hong, and M. C. Asensio, Phys. Rev. B **86**, 115105 (2012).
[23] A. Splendiani, L. Sun, Y. Zhang, T. Li, J. Kim, C.-Y. Chim, G. Galli, and F. Wang, Nano Lett. **10**, 1271 (2010).
[24] A. Kuc, N. Zibouche, and T. Heine, Phys. Rev. B **83**, 245213 (2011).
[25] T. Olsen, K. W. Jacobsen, and K. S. Thygesen, arXiv:1107.0600.
[26] Y. Ding, Y. Wang, J. Ni, L. Shi, S. Shi, and W. Tang, Phys. B **406**, 2254 (2011).
[27] C. Ataca and S. Ciraci, J. Phys. Chem. C **115**, 13303 (2011).
[28] H. Jiang, J. Phys. Chem. C **116**, 7664 (2012).
[29] T. Cheiwchanchamnangij and W. R. L. Lambrecht, Phys. Rev. B **85**, 205302 (2012).
[30] A. Ramasubramaniam, Phys. Rev. B **86**, 115409 (2012).
[31] G. D. Scholes and G. Rumbles, Nat. Mater. **5**, 683 (2006).
[32] S. Ghatak, A. N. Pal, and A. Ghosh, ACS Nano **5**, 7707 (2011).
[33] The transition matrix elements are evaluated from the change of the wave function with respect to **k** vector $\alpha_j = \langle\psi_i| - i\partial/\partial k_j|\psi_f\rangle$, as described in Ref. 58. The radius of the circle in Fig. 1 represents $\alpha_x + \alpha_y$.
[34] G. Kresse and J. Hafner, Phys. Rev. B **47**, 558 (1993).
[35] G. Kresse and J. Furthmüller, Comput. Mater. Sci. **6**, 15 (1996).
[36] J. P. Perdew, K. Burke, and M. Ernzerhof, Phys. Rev. Lett. **77**, 3865 (1996).
[37] T. Böker, R. Severin, A. Müller, C. Janowitz, R. Manzke, D. Voß, P. Krüger, A. Mazur, and J. Pollmann, Phys. Rev. B **64**, 235305 (2001).
[38] S. Grimme, J. Comput. Chem. **27**, 1787 (2006).
[39] The self-consistency via GW_0 approach produces only minor changes (usually less than 0.1 eV increase) in the quasiparticle energies, thereby justifying the G_0W_0 approach. On the other hand, zero-point vibrations would decrease the band gap slightly, and through partial error cancellation, we expect our calculations to provide highly accurate results.
[40] The CBM minimum is at 0.52 between Γ and K. Our indirect gap results are always between the VBM at the Γ point and the CBM at the midpoint between Γ and K.
[41] S. W. Han, H. Kwon, S. K. Kim, S. Ryu, W. S. Yun, D. H. Kim, J. H. Hwang, J.-S. Kang, J. Baik, H. J. Shin, and S. C. Hong, Phys. Rev. B **84**, 045409 (2011).
[42] S. Bhattacharyya and A. K. Singh, Phys. Rev. B **86**, 075454 (2012).
[43] N. Berseneva, A. Gulans, A. V. Krasheninnikov, and R. M. Nieminen (unpublished).
[44] C. Delerue, G. Allan, and M. Lannoo, Phys. Rev. Lett. **90**, 076803 (2003).
[45] P. Cudazzo, C. Attacalite, I. V. Tokatly, and A. Rubio, Phys. Rev. Lett. **104**, 226804 (2010).
[46] L. Wirtz, A. Marini, and A. Rubio, Phys. Rev. Lett. **96**, 126104 (2006).
[47] K. F. Mak, J. Shan, and T. F. Heinz, Phys. Rev. Lett. **106**, 046401 (2011).
[48] V. Perebeinos, J. Tersoff, and P. Avouris, Phys. Rev. Lett. **92**, 257402 (2004).
[49] M. S. Dresselhaus, G. Dresselhaus, R. Saito, and A. Jorio, Annu. Rev. Phys. Chem. **58**, 719 (2007).
[50] K. F. Mak, K. He, J. Shan, and T. F. Heinz, Nat. Nanotechnol. **7**, 494 (2012).
[51] T. J. Wieting and A. D. Yoffe, Phys. Status Solidi B **37**, 353 (1970).

[52] J. Feldmann, G. Peter, E. O. Göbel, P. Dawson, K. Moore, C. Foxon, and R. J. Elliott, Phys. Rev. Lett. **59**, 2337 (1987).

[53] D. Jena and A. Konar, Phys. Rev. Lett. **98**, 136805 (2007).

[54] B. L. Evans and P. A. Young, Proc. R. Soc. London, Ser. A **284**, 402 (1965).

[55] A. R. Beal, J. C. Knights, and W. Y. Liang, J. Phys. C **5**, 3540 (1972).

[56] A. Anedda and E. Fortin, J. Phys. Chem. Solids **41**, 865 (1980).

[57] B. Davey and B. L. Evans, Phys. Status Solidi A **13**, 483 (1972).

[58] M. Gajdoš, K. Hummer, G. Kresse, J. Furthmüller, and F. Bechstedt, Phys. Rev. B **73**, 045112 (2006).

[59] H.-P. Komsa and A. V. Krasheninnikov, J. Phys. Chem. Lett. **3**, 3652 (2012).